The Rich Stereochemistry of Eight-Vertex Polyhedra: A Continuous Shape Measures Study

David Casanova,[a] Miquel Llunell,[b] Pere Alemany,*[b] and Santiago Alvarez*[a]

Abstract: A stereochemical study of polyhedral eight-vertex structures is presented, based on continuous shape measures (CShM). Reference polyhedra, shape maps, and minimal-distortion interconversion paths are presented for eight-vertex polyhedral and polygonal structures within the CShM framework. The application of these stereochemical tools is analyzed for several families of experimental structures: 1) coordination polyhedra of molecular transition-metal coordination compounds, classified by electron configuration and ligands; 2) edge-bonded polyhedra, including cubane structures, realgar, and metal clusters; 3) octanuclear transition-metal supramolecular architectures; and 4) coordination polyhedra in extended structures in inorganic solids. Structural classification is shown to be greatly facilitated by these tools, and the detection of less common structures, such as the gyrobifastigium, is straightforward.

Keywords: continuous shape measures · coordination modes · eight-vertex structures · shape maps · transition metals

Introduction

The use of ideal polyhedra to define the spatial arrangement of a set of atoms is consubstantial with the development of structural chemistry in the 20th century. Such polyhedra can represent, for instance, a group of chemically bonded atoms, as in clusters or cage compounds, a set of ions held together by a Madelung potential and repeated periodically in an extended solid, or bonded to a single atom occupying the center of the polyhedron, as in coordination compounds. Although there are infinite ways in which a given number of atoms can in principle be organized in space, the polyhedral paradigm works surprisingly well in a number of cases. Hence, we tend to describe tetracoordinate transition-metal atoms as tetrahedral or square-planar. We also refer to some polycyclic alkanes as cubanes, prismanes, or dodecahedranes. The organization of molecular building blocks in larger (supramolecular) units is also efficiently represented by polyhedra or polygons of a given set of atoms that are connected by chemical units spanning the edges or the faces, such as the Fe_8 octagons in the so-called iron wheels that exhibit single-molecule magnet behavior. Most of inorganic solid-state materials are described as polyhedra connected in a variety of ways. However, the use of ideal polyhedra is not always straightforward. In many instances a structure deviates significantly from the ideal shapes and the stereochemical descriptions become highly imprecise, for example, slightly distorted octahedron or highly distorted tetrahedron. Furthermore, the assignment of a structure to one of the possible ideal polyhedra is often more a matter of taste than the result of the application of clearly established criteria. Let us take as a further example the descriptions given to the environment of the alkaline earth cations in the garnet structures: as noted by O'Keeffe and Hyde,[1] different authors have referred to a "skew cube", a "distorted square antiprism", and a "distorted dodecahedron". How can the same structure be described by three polyhedra that are quite different in symmetry and in terms of interatomic distances? The problem of assigning an ideal polyhedron to a structure increases with increasing number of atoms, since the number of available polyhedra increases, and they differ from each other in smaller atomic displacements.

[a] D. Casanova, Prof. S. Alvarez
Departament de Química Inorgànica and
Centre de Recerca en Química Teòrica
Universitat de Barcelona
Diagonal 647, 08028 Barcelona (Spain)
Fax: (+34) 93-490-7725
E-mail: santiago@qi.ub.es

[b] Dr. M. Llunell, Dr. P. Alemany
Departament de Química Física and
Centre de Recerca en Química Teòrica
Diagonal 647, 08028 Barcelona (Spain)
Fax: (+34) 93-402-1231
E-mail: alemany@qf.ub.es

 DOI: 10.1002/chem.200400799

Following the proposal of Avnir et al.[2,3] that symmetry and polyhedral shape can be defined in terms of continuous properties that can be quantified from structural data, we have developed a project aimed at evaluating the applicability of such continuous symmetry measures (CSM) and continuous shape measures (CShM) to inorganic systems. The usefulness of these measures for the stereochemical analysis of very large sets of molecular structures has been shown so far for the cases of four-,[4] six-,[5] and seven-vertex[6] polyhedra. Also a new way to define at a quantitative level those structures that are in-between two reference polyhedra has been developed by the definition of minimal distortion interconversion pathways and the corresponding path deviation functions.[7] The previous results have encouraged us to undertake a broad study of eight-vertex chemical structures, which are usually difficult to analyze and for which general stereochemical studies were reported more than two decades ago.[8–11] More recent reviews mostly concentrate on the description of the characteristic eight-vertex polyhedra and analyze a limited set of experimental structural data.[12,13] Incorporation of more recent structural data together with application of CShM thus seemed timely. Here we present first a brief summary of the CShM concepts and methodology. Then we present the collection of ideal eight-vertex polyhedra used for our stereochemical study and discuss the criteria adopted for our choice of ideal reference shapes. Then we report the results of applying our method to different families of eight-vertex chemical structures: 1) transition-metal coordination compounds, analyzed by electron configuration and by families according to ligands; 2) edge-bonded polyhedra, including cubane structures, the polyhedra associated with the structure of realgar, and metal clusters; 3) octanuclear transition-metal supramolecular architectures; and 4) extended structures in inorganic solids.

Abstract in Catalan: *En aquest article es presenta un estudi estereoquímic d'estructures amb vuit vèrtexs basat en les mesures contínues de forma (CShM). Es presenten els políedres de referència, els mapes de forma i els camins d'interconversió de mínima distorsió per a estructures polièdriques i poligonals amb vuit vèrtexs, dins el marc de les CShM. S'analitza l'aplicació d'aquestes eines estereoquímiques a diverses famílies d'estructures experimentals: (a) políedres de coordinació en compostos moleculars de metalls de transició, classificats tant per configuració electrònica del metall com per tipus de lligands; (b) políedres amb enllaços a les arestes, incloent estructures de tipus cubà, clústers metàl·lics i el realgar; (c) arquitectures supramoleculars octanuclears de metalls de transició i (d) políedres de coordinació en estructures infinites de sòlids inorgànics. La classificació estructural es facilita molt mitjançant l'ús d'aquestes eines, i la detecció d'estructures poc comunes, com ara el girobifastigi és immediata.*

Results and Discussion

Continuous shape measures: The continuous symmetry (CSM) and shape (CShM) measures proposed by Avnir et al.[2,14] essentially allow one to numerically evaluate by how much a particular structure deviates from an ideal symmetry or from an ideal shape (e.g., a polyhedron). The CShM relative to a polyhedron P for a set of N atoms (in the present case $N=8$ for empty polyedra and $N=9$ for centered polyhedra), characterized by their position vectors Q_i, is defined by Equation (1), where P_i is the position vector of the corresponding vertex in the reference polyhedron P, and Q_0 the position vector of the geometrical center of the problem structure.

$$S_Q(P) = \min \frac{\sum_{i=1}^{N} |Q_i - P_i|^2}{\sum_{i=1}^{N} |Q_i - Q_0|^2} 100 \qquad (1)$$

The minimum is taken for all possible relative orientations in space, isotropic scaling, and for all possible pairings of the vertices of the problem and reference polyhedra. As a consequence, two shapes are identical within the CShM approach if they differ only in size and/or orientation in space. For the study of coordination compounds, only those vertex permutations that leave the metal atom in the center of the polyhedron are considered. With such a definition, $S_Q(P)=0$ corresponds to a structure Q fully coincident in shape with the reference polyhedron P, whereas the maximum allowed value is $S_Q(P)=100$, which corresponds to the hypothetical case in which all atoms of Q occupy the same point in space.

Although we have referred so far to a methodology that can be applied to the calculation of symmetry or shape measures, we must be aware of the analogies and differences between shape and symmetry. Such a difference becomes clear if we consider a polyhedron for which the symmetry does not fully determine its geometry, as for the hexagonal bipyramid. We show three such bipyramids **1a–1c** that differ in the ratio between width and height but all have full D_{6h} symmetry. For those cases in which the choice of a reference polyhedron with a given symmetry is not unique, we actually have two choices for the definition of its P_i coordinates: either we search for the nearest polyhedron that has the desired symmetry or we establish a conventional poly-

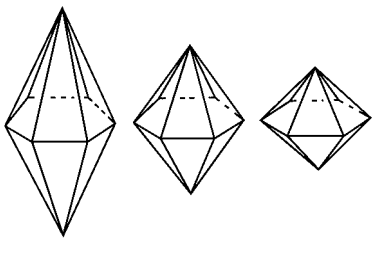

1a **1b** **1c**

hedron relative to which we calculate the measures according to Equation (1). The CSM is $S(D_{6h})=0$ for **1a**–**1c**. On the other hand, if we choose one of those bipyramids (e.g., **1b**) as our conventional polyhedron (let us call it **HBPY**), then we obtain a CShM. The resulting shape measure S(HBPY) will be zero only for the conventional bipyramid, but nonzero for the other two bipyramids **1a** and **1c**. A bipyramid that can be made coincident with the conventional one by translation, rotation, or isotropic scaling will have S(HBPY)=0, that is, it has the same shape. Since the shape criterion is in general more restrictive than the symmetry approach, it has been found adequate in the case of eight-vertex polyhedra to define conventional reference polyhedra and use the corresponding shape measures throughout this paper. However, for two eight-vertex geometries, shape and symmetry are equivalent, and these are the cube and the regular octagon.

Another example of this behavior is the relationship between the dodecahedron (**DD**) and the snub disphenoid (**SD**). Both have the same symmetry (D_{2d}), but their shapes are different. Then, the CSM from D_{2d} is zero for the two structures, but the CShM from one to the other is nonzero ($S_{DD}(SD)=S_{SD}(DD)\neq 0$).

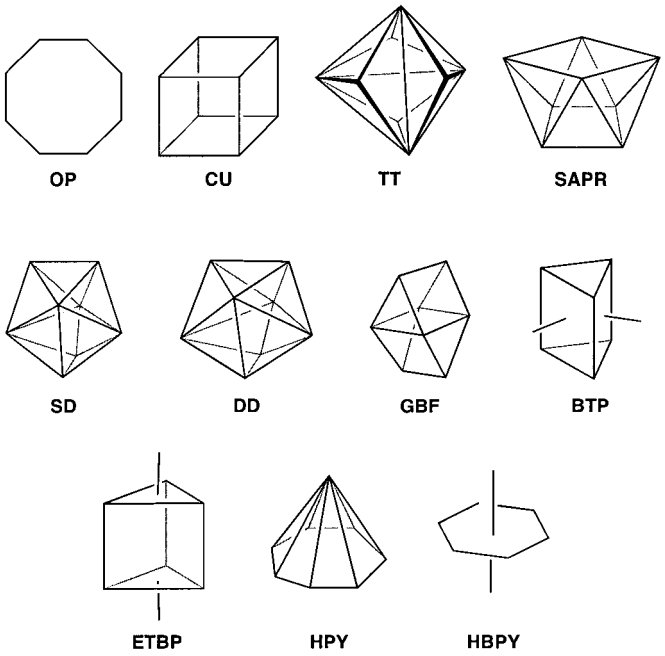

Scheme 1.

Eight-vertex reference polyhedra: The first step of our stereochemical study aimed at assigning an ideal polyhedral geometry to specific groups of atoms is perforce to define the reference polyhedra (including the planar polygons). From previous work, we have found it useful to consider as ideal shapes the regular polygons, the Platonic solids, the Archimedean polyhedra, the prisms, and the antiprisms.[15] All other polyhedra (92 in total) having regular polygons as faces and between 5 and 75 vertices are known as Johnson polyhedra[16] and are also useful as stereochemical descriptors, even if they are far less commonly used. The corresponding shapes with eight vertices are schematically represented in Scheme 1, together with the abbreviations used throughout this paper. We present a relatively large number of polyhedra here not just for comprehensiveness, but because it will be seen below that one can find examples of chemical structures for each of these shapes with the exception of the heptagonal pyramid. The main characteristics of our ideal shapes, summarized in Table 1, are briefly discussed here.[17]

Table 1. Names, abbreviations, and main characteristics of the ideal eight-vertex polyhedra used as references in this work. The prefix **J**- indicates a Johnson polyhedron, and the prefix **s**- indicates the spherical version of the corresponding polyhedron.

Ideal shape	Abbreviation	Symmetry	Regular faces	Equiv faces	Spherical	Equiv edges
octagon	**OP**	D_{8h}	–	–	yes	yes
cube	**CU**	O_h	yes	yes	yes	yes
triakis-tetrahedron	**TT**	T_d	no	yes	no	no
square antiprism	**SAPR**	D_{4d}	yes	no	yes	yes
snub disphenoid	**J-SD**	T_d	yes	yes	no	yes
triangular dodecahedron	**DD**	D_{2d}	no	no	imposed	no
gyrobifastigium	**J-GBF**	D_{2d}	yes	no	no	yes
biaugmented trigonal prism	**J-BTP**	C_{2v}	yes	no	no	no
	s-BTP	C_{2v}	no	no	imposed	no
elongated trigonal bipyramid	**J-ETBP**	D_{3h}	yes	no	no	no
	s-ETBP	D_{3h}	no	no	imposed	no
heptagonal pyramid	**HPY**	D_{7h}	no	no	imposed	no
hexagonal bipyramid	**HBPY**	D_{6h}	no	no	imposed	no

The regular octagon (**OP**), the cube (**CU**), and the triakis-tetrahedron (**TT**) are univocally defined shapes, as determined by their symmetries (D_{8h}, O_h, and T_d, respectively) and, in the last-named case, by the condition of being the dual of the truncated tetrahedron. The triakis tetrahedron has the shape shown in **2a**–**2c**, with 12 faces and 18 edges and is a nonconvex polyhedron having two types of vertices at different distances from the geometrical center, the ratio between the long and short distances being 1.218. This polyhedron can be described as resulting from capping each face of a tetrahedron (**2a**), but also as resulting from the super-

position of two tetrahedra with a common center (**2b**) or as a distorted cube (**2c**).

Other ideal polyhedra are univocally defined if we require all their faces to be regular polygons (i.e., all edges of the same length, coincident with the definition of the Johnson polyhedra), as is the case for the square antiprism (**SAPR**). The ideal **SAPR** adopted here (**3**), coincident with that of a

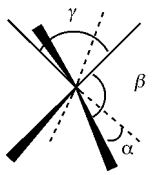

3

hard-spheres model, has twelve identical L–L distances ($d_{L-L}=1.215\,d_{M-L}$), and its edges subtend angles with the geometric center of $\alpha=74.85$, $\beta=85.48$, and $\gamma=119.52°$. In other cases, though, this condition implies that the polyhedron cannot be spherical (i.e., the distances from the vertices to the center of the polyhedron are not all equal), as in the gyrobifastigium (**GBF**), the snub disphenoid (**SD**), and the Johnson bicapped trigonal prisms (**BTP** and **ETBP**, named biaugmented trigonal prism and elongated trigonal bipyramid, respectively). For these polyhedra it is useful to have at hand two versions: a Johnson nonspherical polyhedron (identified by the prefix **J-**) and a spherical one with nonequivalent edges (labeled with the prefix **s-**). The snub disphenoid (**SD**) is a 12-face convex deltahedron, also known as Siamese dodecahedron. The gyrobifastigium (**GBF**), one of the Johnson polyhedra, is an octahedron that can be described as formed by fusing together two triangular prisms through a square face, but rotated by 90° in such a way that their trigonal axes are orthogonal. Both **BTP** and **ETBP** can be thought of as trigonal prisms with two additional vertices, on the center of two square faces in the biaugmented trigonal prism (**BTP**) and on the center of the two triangular faces in the elongated trigonal bipyramid (**ETBP**).

The third set of ideal shapes is constituted by polyhedra on which we arbitrarily impose sphericity (all vertices at the same distance from the center) while keeping the corresponding topology and symmetry. These are the hexagonal bipyramid (**HBPY**), the triangular dodecahedron (**DD**, the spherical version of the snub disphenoid), and the spherical versions of the Johnson bicapped trigonal prisms (**s-BTP** and **s-ETBP**). In the case of the triangular dodecahedron, sphericity and symmetry are not enough to provide an unambiguous definition, and we therefore adopted the geometry that corresponds to a hard-spheres model. The dodecahedron has the same topology and symmetry (D_{2d}) as the snub disphenoid. However, the dodecahedron is spherical, while the snub disphenoid is not, and the faces of the former are nonregular triangles, whereas those of the latter are equilateral triangles. The CShM of the **SD** and the **DD** relative to each other, $S_{SD}(DD)=2.85$, gives us a quantitative idea of the significant difference between these two shapes, in spite of their identical topology and symmetry. In the case of the heptagonal pyramid (**HPY**) we arbitrarily impose the restriction that the central atom, if present, lies in the basal plane.

Shape maps and interconversion pathways: In a CShM structural analysis of a given molecule, we can compare the measures obtained with respect to the different ideal polyhedra and decide which of them best describes the molecular geometry by just choosing the smallest CShM value. This numerical value also gives an indication of how distorted the structure is from the reference shape. Let us consider as simple examples the coordination polyhedra formed by the metal and donor atoms in the following compounds: the purely organometallic[18] $[Re(CH_3)_8]^{2-}$, the anionic complex $[Y(hfacac)_4]^-$ (hfacac = hexafluoroacetylacetonate),[19] and $[W(CN)_8]^{4-}$ in its hydrated bipyridinium salt.[20] The shape measure of the first complex relative to the square antiprism is 0.21, whereas its measures relative to the dodecahedron and the bicapped trigonal prism are 2.33 and 2.89, respectively, and those relative to the other reference polyhedra are even significantly larger, so we can identify this coordination polyhedron unequivocally as a square antiprism. In the second case, $S(DD)=0.18$, while $S(SAPR)=1.94$ and other shape measures are even larger, that is, the coordination sphere is clearly dodecahedral. Finally, the octacyano complex has rather similar values of the shape measures relative to the dodecahedron and the square antiprism (0.75 and 0.88, respectively), and values larger than 2.4 for other reference shapes, and this precludes a clear description of its geometry as either **DD** or **SAPR**. However, if we calculate the deviation of such a molecule from the **DD–SAPR** interconversion path, we obtain a rather small value (0.06) that allows us to describe its coordination polyhedron as intermediate between these two reference shapes.

To be more precise, we should be able to tell not only by how much, but also in which direction, the geometry is distorted. Two tools can be of help for that task. One consists of representing the CShM data in scatterplots of the shape measures relative to two ideal polyhedra, which we have named shape maps.[5] Since specific distortions appear in the shape maps as well-defined lines, the position of a given molecule in the shape map offers us good hints to the likely distortion, although this technique does not always give an unequivocal description of the distortion. The other tool, the path deviation functions defined by us recently,[7] indicates whether a molecular structure lies along the path for interconversion between two polyhedra or, more precisely, by how much it deviates from that path. The use of shape maps and path deviation functions to describe distortions from ideal geometries provides us an alternative to geometrical descriptions in terms of angles and bond lengths. Even if we are more familiar with the latter method, the description of distortions in terms of the distance from two ideal shapes is no less intuitive and has some advantages: 1) In some cases for which a single angular parameter describes a geometrical distortion pathway (e.g., the square–tetrahedron

interconversion) the shape measures approach is equivalent.[7] 2) The CShM approach allows us to compare on the same scale distortions of a given structure toward different shapes, for instance, a Bailar twist and a tetragonal Jahn–Teller distortion in a hexacoordinate complex. 3) It also allows us to compare distortions of the coordination spheres of molecules with different numbers of vertices, for example, it shows that the spread pathway connecting the square and the tetrahedron is equivalent to the interconversion of the cube and the octagon.[7] 4) Distortions that cannot be easily described in terms of a single geometrical parameter or whose distortion coordinates are not so intuitive (e.g., the interconversion of the eight-vertex triangular dodecahedron and the cube) are nicely described in terms of shape measures. In this section we briefly describe two shape maps for eight-vertex polyhedra and the corresponding path deviation functions.

For the eight-vertex polyhedra, the CShMs of each reference polyhedron relative to the others are given in Table 2. Furthermore, their CShM values relative to the cube and to the square antiprism are represented in a shape map (Figure 1, top). In both cases we can see that the dodecahedron, the snub disphenoid, the square antiprism, and the bicapped trigonal prism are very close to each other. Also separated by small distances are two related shapes, the cube and the triakis tetrahedron. The rest of the distances between reference polyhedra are rather large. In particular, each of the following figures is quite far from all other shapes: **HBPY**, **HPY**, **GBF**, **ETBP**, and **OP**. Interestingly, the difference between the spherical and Johnson versions of the bicapped trigonal prism, **J-BTP** and **s-BTP**, is reflected in a nonnegligible CShM value of these polyhedra relative to each other (1.439). Such a difference is still more pronounced between the **J-ETBP** and **s-ETBP** ideal polyhedra (CShM of 6.578).

In Figure 1 we can also represent the paths for polyhedral interconversion, either obtained by imposing a certain geometrical distortion on a molecular model or through the minimal distortion paths[7] described below. Note that in the **SAPR–CU** map those structures occupying the positions of the square antiprism (S(SAPR)=0) or of the cube (S(CU)=0) can be unequivocally identified with those ideal polyhedra. However, a structure that occupies the position

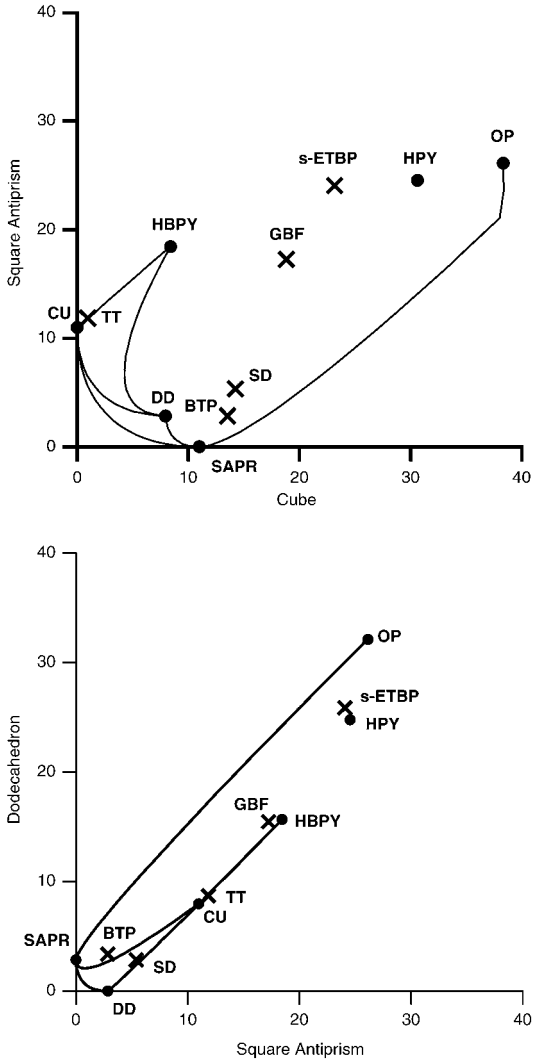

Figure 1. Shape map in the cube–square antiprism space (top) and in the square antiprism–dodecahedron space (bottom), the positions that the ideal polyhedra (Scheme 1) occupy in those maps, and some of their interconversion paths.

corresponding to another ideal polyhedron in the shape map does not necessarily correspond to that polyhedron. Hence, we need to verify that the CShM corresponding to that ideal

Table 2. Reciprocal shape measures between reference eight-vertex polyhedra (see Scheme 1 and Table 1 for drawings and names).

	SD	SAPR	J-BTP	CU	TT	HBPY	GBF	J-ETBP	HPY	OP
DD	2.847	2.848	3.361	7.952	8.686	15.678	15.461	30.496	24.794	32.135
SD	0	5.362	3.002	14.257	12.669	19.555	10.049	25.962	27.215	30.131
SAPR		0	2.843	10.989	11.838	18.458	17.259	28.515	24.535	26.120
J-BTP			0	13.507	13.073	18.594	13.674	24.959	25.397	28.258
CU				0	0.953	8.395	18.811	25.086	30.612	38.311
TT					0	9.260	19.536	25.675	29.983	38.883
HBPY						0	11.014	27.195	23.666	32.421
GBF							0	25.274	27.472	35.766
J-ETBP								0	26.937	34.936
HPY									0	22.809
OP										0

polyhedron is close to zero before making such a stereochemical assignment. In the same way, the fact that the cube appears along the path between the dodecahedron and the hexagonal bipyramid in the **DD–SAPR** map (Figure 1, bottom) does not necessarily mean that the interconversion between the dodecahedron and the hexagonal bipyramid passes through a cubic shape, since we are looking at a two-dimensional map of geometrical data in a $3N$-dimensional space.

Note that a wide variety of shape maps are available to us, as many as the pairs of reference polyhedra we can choose, or 55 different maps in the present case considering the 11 shapes presented in Scheme 1. As in real life, we use the map that best describes the region we wish to explore, that is, the one related to the two most common shapes for the set of structures we are analyzing. Thus, in this work we use essentially the dodecahedron–square antiprism map (see discussion and Figure 5 below), although in specific cases two other maps will be used.

The minimal distortion pathways between two reference shapes can be defined in terms of CShMs.[7] Thus, we can determine how close a given structure is to an interconversion pathway if we know its shape measures relative to the two reference polyhedra. This is done by calculating the path deviation function presented in Equation (2), which determines the degree of deviation of structure X from the minimal distortion interconversion pathway between reference shapes P and T. The values of the mutual shape measures between pairs of ideal polyhedra $S_P(T)$ are presented in Table 2.

$$\Delta_X(P,T) \equiv \frac{1}{\arcsin\frac{\sqrt{S_P(T)}}{10}}\left[\arcsin\frac{\sqrt{S_X(P)}}{10}+\arcsin\frac{\sqrt{S_X(T)}}{10}\right]-1 \quad (2)$$

Transition-metal coordination compounds: an overview: The experimental data analyzed in this section were retrieved from the Cambridge Structural Database[21] (CSD, version 5.25) by searching for compounds with a metal atom defined in the database as octacoordinate and belonging to Groups 3–12 for which the following restrictions were applied: no π-bonded ligands were allowed and structures with disorder or with agreement factors R greater than 10% were disregarded. As donor atoms we included all elements of Groups 14–17 and hydrogen. A total of 501 compounds were found, comprising 531 crystalographically independent structural data sets. The distribution of those compounds along the transition-metal series is shown in Figure 2. Octacoordination is most common for early transition metals (Groups 3–7) of the second and third series and for the heavier elements of the Zn group, and Zr is the most common octacoordinate transition metal.

A bird's-eye view of the relative importance of the different ideal polyhedra in octacoordinate transition-metal complexes can be gained by looking at the shape map obtained from a scatterplot of the CShMs of the experimental structures relative to the dodecahedron and the square antiprism (Figure 3, bottom). We first note that some regions of the map, delimited by lines corresponding to some of the studied distortions, are geometrically forbidden, as previously discussed for tetracoordinate compounds.[4] By comparison with the position of the ideal structures in a similar shape

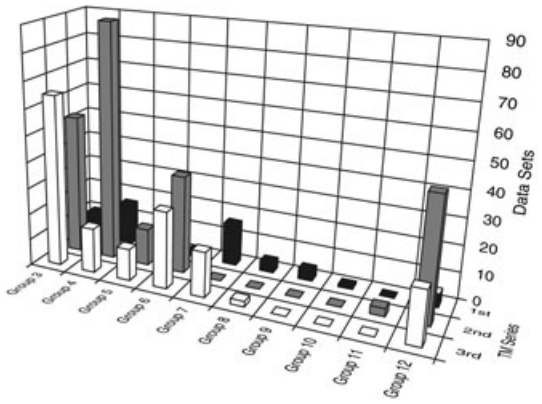

Figure 2. Periodic distribution of octacoordinate transition-metal complexes in the CSD.

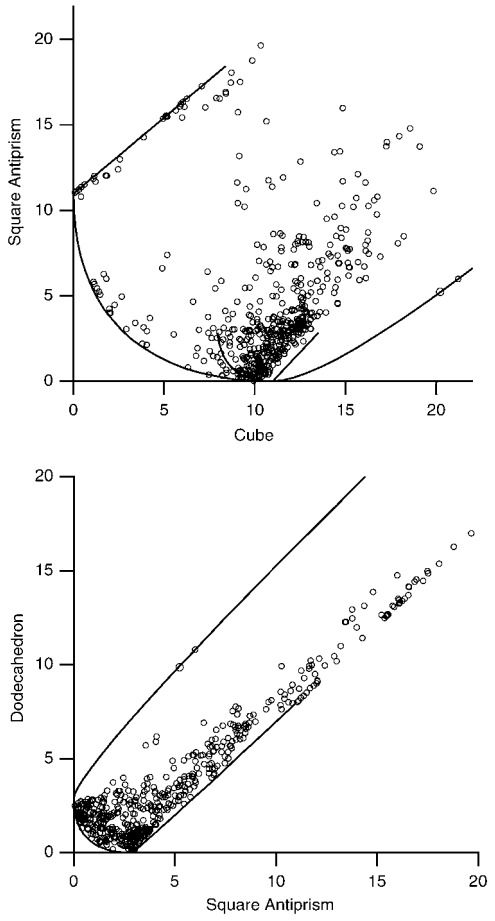

Figure 3. Location of the transition-metal octacoordinate complexes retrieved from the CSD in two shape maps. The continuous lines correspond to polyhedra interconversion paths identified in Figure 1.

map (Figure 1) we see that the most common shapes are in the region around the **SAPR**, the **DD**, and the **BTP** (the lower left corner of the map), although a good number of structures appear along the rightmost branch of the map, which was seen (Figure 1, bottom) to correspond to distortions from the dodecahedron toward the cube or hexagonal bipyramid. Moreover, no structures correspond to the heptagonal pyramid or octagon. However, two points at the leftmost part of the **DD-SAPR** map, clearly differentiated from the rest of the structures, appear right in the middle of the flattening pathway that leads from the square antiprism to the planar octagon, to be discussed below. The most salient feature of these shape maps is that most structures are found at a significant distance from the ideal polyhedral shapes; hence, the polyhedron that best describes each geometry cannot be assigned on the basis of only one specific shape map, and we should perform a more detailed analysis to obtain some idea about the relative importance of the less common shapes.

Several ideal eight-vertex structures were classified by Muertterties and Wright[8] into two groups: low-energy structures (**DD**, **SAPR**, and **BTP**) and high-energy structures (**ETBP**, **CU**, **HPY**, and **HBPY**). This classification is consistent with the electrostatic repulsion coefficients given by Kepert,[10] which indicate much less ligand–ligand repulsion for the first three polyhedra, and is also in agreement with a d orbital energy scheme obtained from the angular overlap model[22] (AOM) shown in Figure 4. Optimum involvement of d orbitals in metal–ligand bonding occurs for these three structures and leaves at most one d orbital as nonbonding, whereas for the rest of the shapes two d orbitals cannot be involved in metal–ligand bonding for reasons of symmetry and are therefore nonbonding. The distribution of coordination polyhedra found among octacoordinate transition-metal complexes seems to confirm that the dodecahedron, the square antiprism, and the bicapped trigonal prism are energetically favored, and from here on we will refer to these shapes as low-energy shapes, though only when referring to coordination compounds.

We can assign the polyhedron that best describes the coordination sphere of the octacoordinate metal atom in each compound by calculating their CShMs relative to the various polyhedra in Scheme 1 and thus obtain a perspective view of the stereochemical preferences of experimental structures. Among the structures that are significantly distant from the ideal shapes, we are still able to identify many as being very close to the interconversion path between two such shapes, according to the path deviation functions described above.

Since we have seen (Table 2) that the distances between the low-energy eight vertex polyhedra (**DD**, **SAPR**, and **BTP**) are rather small compared to the distance between these and the rest of the polyhedra, we have classified the structures first as belonging to either the region of the low-energy polyhedra or to that of the other polyhedra, within a CShM of 2.0. The structures that remain unclassified are then analyzed to see if they are adequately described as lying along a given polyhedral interconversion path, with a tolerance of $\Delta(\text{path}) \leq 0.5$. The structures belonging to the low-energy region of the shape map can then be assigned to one of the low-energy polyhedra with a more stringent criterion ($S(\text{polyhedron}) \leq 0.7$) than for the other polyhedra, or to one of their interconversion paths (within $\Delta(\text{path}) \leq 0.3$). Once all these structures have been classified, we are left with 12.9% of unassigned structures that can be adequately described neither by one of the polyhedra under consideration nor as lying along their interconversion paths. The tolerance factors that we have applied for our classification scheme are somewhat arbitrary, and the actual portion of structures assigned to each polyhedron or interconversion path can vary with a different choice. However, we obtain a quite interesting qualitative picture (Figure 5) that is not significantly affected by the numerical criteria used.

According to the distribution shown in Figure 5, several interesting observations can be made: 1) A relatively small number of structures can be unambiguously described as do-

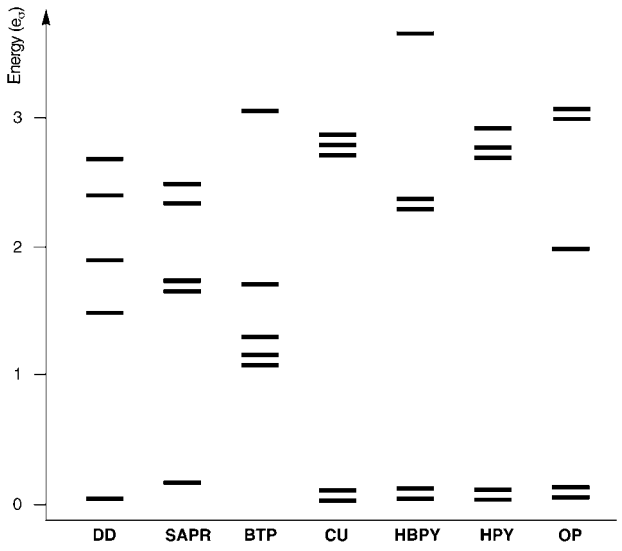

Figure 4. Energy diagram for the d orbitals in octacoordinate environments, as predicted by the angular overlap model (up to second order). Standard e_σ units are used for the orbital energies.

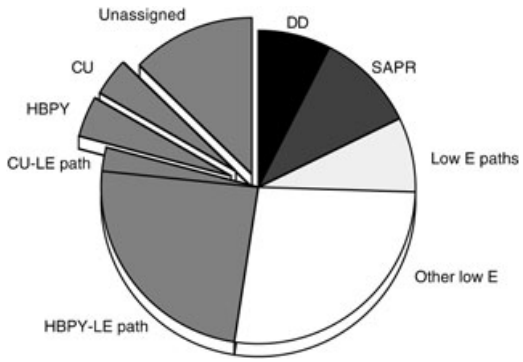

Figure 5. Distribution of eight-vertex polyhedra among transition-metal coordination compounds. LE refers to the "low-energy" polyhedra (**DD**, **SAPR**, and **BTP**); for the other abbreviations, see Scheme 1.

decahedral or square-antiprismatic (7.5 and 10.4%, respectively, with the numerical criteria applied here), while only one bicapped trigonal-prismatic structure was found within the tolerance margin adopted. 2) These low-energy structures together with intermediate geometries (labeled "other low E" in Figure 5) and their distortions along polyhedral interconversion paths represent a majority of the analyzed compounds (a total of 52.7%). 3) A substantial number of structures are best described as being along the paths from the hexagonal bipyramid to the low-energy structures (24.1%). 4) A small but nonnegligible fraction of the structures can unambiguously be identified as cubes (3.8%) or as hexagonal bipyramids (4.1%).

We also analyzed the polyhedral distribution of the data set of transition-metal complexes by electron configuration. As expected from the distribution throughout the periodic table discussed above (Figure 2), we found that the most common configuration among octacoordinate compounds is d^0. Significant numbers of compounds are also found for d^1, d^2, and d^{10} configurations, while only a few examples are found for the remaining d^n configurations. The d^0 to d^2 configurations exhibit similar stereochemical behavior, with most of the structures in the region corresponding to **SAPR**, **DD**, **BTP**, and their interconversion paths, as illustrated in Figure 6a for the case of d^0 compounds, although a few nearly cubic structures are also found with this configuration (leftmost portion of Figure 6a) that correspond to $[Y^{III}L_2]$ and $[La^{III}L_2]$, where L is a tripod[23] or a tetradentate macrocyclic ligand.[24] That many structures fall along the **SAPR**–**DD** interconversion pathway can be seen in the corresponding map for the d^1 compounds (Figure 6b). The trends found for complexes of the d^{10} ions are clearly different from those of the early transition metals (Figure 6c): 1) nearly half of the structures correspond to geometries along the **CU**–**SAPR** interconversion pathway, 2) some 26% of the structures can be classified as hexagonal bipyramids, and 3) no dodecahedral structures appear in the d^{10} family.

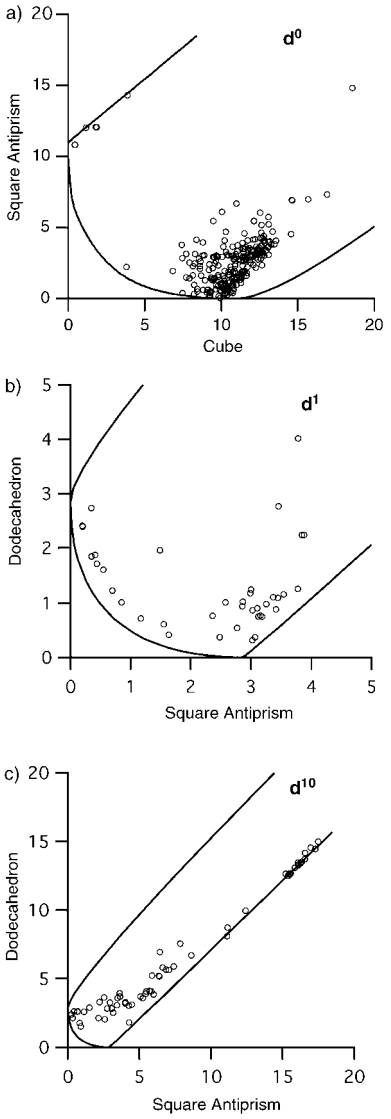

Figure 6. Shape maps for transition-metal coordination complexes with different electronic configurations a) d^0, b) d^1, and c) d^{10}. The lines shown in the square antiprism–cube map correspond (from left to right) to the **CU**–**HBPY**, **CU**–**SAPR**, and **SAPR**–**OP** interconversion paths, whereas those in the dodecahedron–square antiprism maps correspond to the **SAPR**–**OP**, **SAPR**–**DD**, and **DD**–**CU-HBPY** paths (see Figure 1).

Stereochemical preferences due to ligands

Transition-metal octacyano complexes: A good example of the structural variability of octacoordinate complexes in the absence of constraints imposed by bi- or multidentate ligands is provided by the family of octacyano complexes.[13] The sample of octacyano complexes analyzed by us is composed of 59 structural data sets of 53 compounds of Mo^{IV}, Mo^{V}, W^{IV}, W^{V}, Nb^{III}, and Nb^{IV}. Their stereochemical behavior is best appreciated in the **SAPR**–**DD** shape map (Figure 7a). The molecular structures of these cyano complexes cover practically the entire interconversion path between these two polyhedra, and is summarized by their calculated deviation functions (Figure 7b).

Bidentate ligands: We have analyzed the homoleptic complexes of bidentate ligands **4**–**6** of general formula $[M(chel)_4]$ (chel = nitrate, dithiocarbamate, oxalate, or β-diketonate), for which the number of crystallographically independent octacoordinate metal atoms found were 12, 41, 7, and 77 (in the last case including non-transition metals), respectively. The results for these compounds can be best visualized in the **DD**–**SAPR** shape map (Figure 8). The biden-

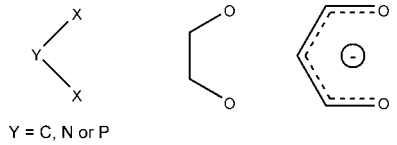

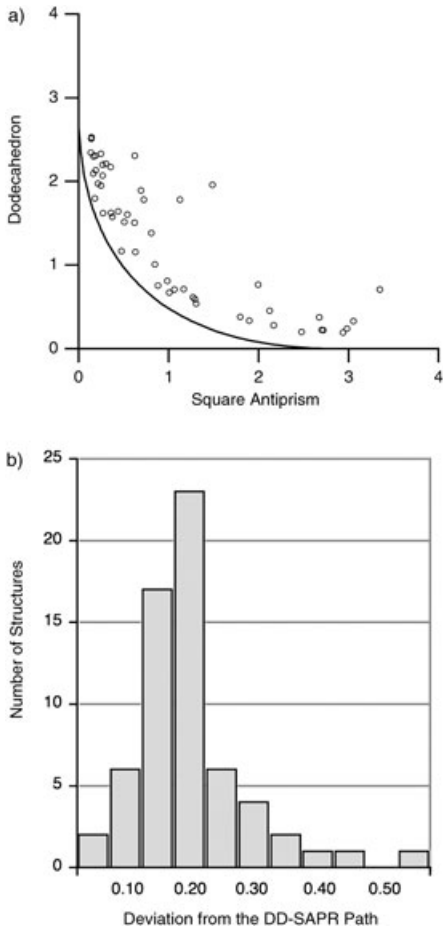

Figure 7. Shape measures of octacyano complexes in the **DD–SAPR** shape map (a) and histogram of their deviation functions from the **DD–SAPR** minimal distortion interconversion path (b).

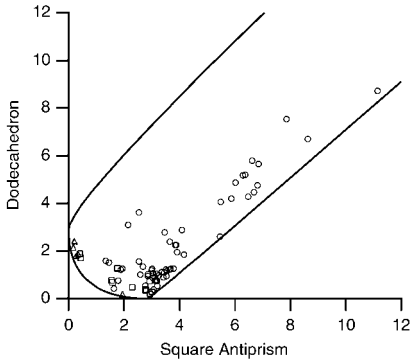

Figure 8. Shape map for tetrakis(didentate) complexes relative to the dodecahedron and the square antiprism. The continuous lines shown correspond (from left to right) to the **SAPR–OP**, **SAPR–DD**, and **DD–CU-HBPY** interconversion paths. ○: small-bite bidentate ligands **4**; □: ligands with topology **5**; and △: β-diketonates **6**.

tate ligands with larger bites (β-diketonato **6** and oxalato **5** with normalized bites of 1.41 and 1.31, respectively, with metals of the first transition series) appear in complexes with dodecahedral, square antiprismatic, and intermediate geometries. The complexes with the smaller ligands **4**, such as dithiocarbamato or nitrato (normalized bites of 1.21 and 0.96), however, appear in dodecahedral structures, albeit significantly distorted in most cases toward the cube because of the small size of the edges spanned by the bidentate ligands, and eventually reaching the cube in two cases that correspond to the central Co atom in two nonanuclear compounds,[25] coordinated by the doubly deprotonated form of di-2-pyridyl ketone, $[(2\text{-}C_5H_5N)_2CO_2]^{2-}$, with shape measures relative to the cube of 1.66 and 1.82.

Tripod ligands: Complexes with tripod ligands, $[M(tripod)_2]$, with the same topology as those of **7a**–**7b** are relatively common (49 structural data sets found). The most common

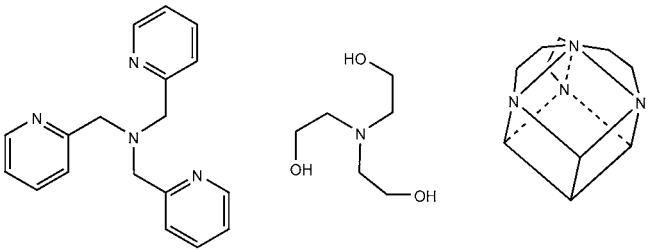

7a **7b** **7c**

shape here is the dodecahedron (76%), but cubic structures are also frequent (22%), probably due to the fact that the trigonal symmetry of these tripods is well adapted to span three neighboring edges of the cube with a common vertex occupied by the apex of the tripod (**7c**).

Bis(tetradentate macrocycle) complexes: In the complexes with two tetradentate phthalocyaninato (skeleton as in **8** with X=N) or porphyrinato (**8** with X=CH) ligands, even if the macrocyclic ligands are significantly corrugated, their four N donor atoms remain coplanar, and thus sandwich structures result that can in principle be cubic (eclipsed conformation of the two ligands), square antiprismatic (staggered conformation), or square metaprismatic (with any intermediate rotation angle). The cubic and square antiprismatic shape measures for the molecular structures of such

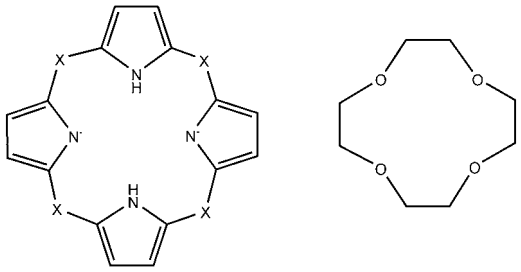

8 **9**

compounds are very close to **SAPR**, in some cases slightly distorted along the tetragonal axis. In the case of the analogous sandwich complexes with the O_4 crown ligand **9**, the results are similar in spite of the enhanced flexibility of the ligand.

Complexes with hexadentate crown ethers: The hexadentate O_6-crown ligands **10** can in principle occupy six nearly coplanar coordination positions and allow two additional ligands to coordinate at axial positions in $[M(O_6\text{-crown})L_2]$ compounds with hexagonal-bipyramidal structure. This is what is found according to their small **HBPY** shape measures, which lie in the range $0.2 < S(\text{HBPY}) < 1.6$ (16 structures of 13 Hg^{II} and Cd^{II} compounds).

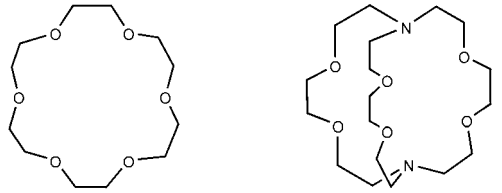

10 **11**

Octadentate encapsulating ligands: The trigonal symmetry of the [2.2.2]cryptand ligand **11** is suitable for either an elongated trigonal bipyramid (**ETBP**) or a cube, the latter requiring a twisted ligand to provide a cubic geometry of the donor atoms. Three such structures were found for complexes of Hg^{II}, Cd^{II}, and Mn^{II} with octadentate [2.2.2]cryptand ligand **11**,[26–28] and they all have nearly cubic geometries with shape measures of 0.07,[28] 0.16,[3] and 1.09,[26] respectively.

Tentacular octadentate ligands: We include in this category ligands with a tetradentate macrocyclic skeleton that extends four tentacles with a donor atom at each end. Examples are the calixarenes **12** and derivatives of tetraaza macrocycles such as **13**. All coordination compounds with these ligands (9 structures with ligand **12**, 27 structural data sets of 21 compounds with ligand **13**), including those of non-transition metal ions (e.g., rare earths, Na^+, Pb^{2+}, or Bi^{3+}) have

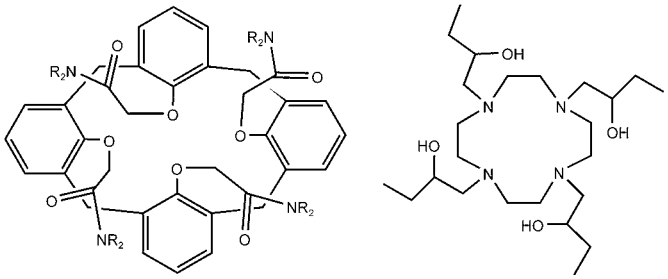

12 **13**

geometries that are rather close to the interconversion path between the cube and the square antiprism, as revealed by their path deviation functions ($\Delta = 0.08$ for **13**, $0.08 \leq \Delta \leq 0.32$ for **12**).

Summary of stereochemical preferences by ligand: The trends found for the families of complexes with the ligands analyzed are schematically summarized in Figure 9, where a

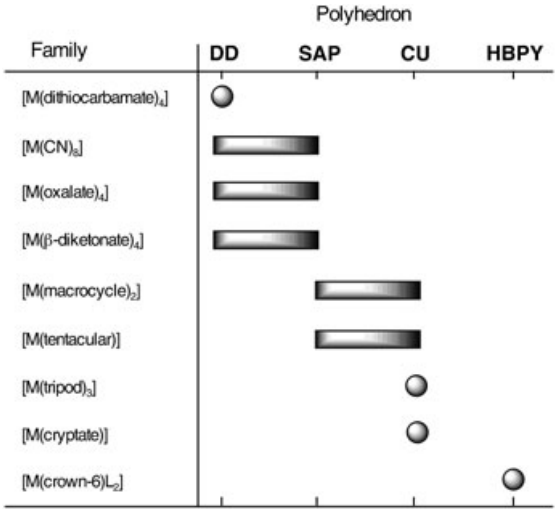

Figure 9. Preferred polyhedra for different families of octacoordinate transition-metal complexes, grouped by ligands. A circle indicates the preferred polyhedron, a bar indicates that structures are found for the two polyhedra at the extremes and for intermediate geometries along the interconversion path.

circle indicates a preferred polyhedron and a bar indicates that structures are found along the path between the corresponding polyhedra. However, the result for the cryptate family should be treated with caution because of the small number of structures found.

Less common structures: Among the structures that appear far from the common ideal polyhedra, our shape maps have allowed us to detect some special cases. Two interesting examples are $[CeCl_4(NO_3)_2]^{2-}$ and $[Cd(NO_3)_4]^{2-}$,[29] which have gyrobifastigium geometries. Even though the corresponding CShM values are not small (4.29 and 4.34, respectively), the large distance between **GBF** and all other ideal eight-vertex polyhedra (Table 2) makes the assignment of this shape unequivocal, as can be appreciated in a perspective view of the molecular structure of the latter (Figure 10), in which its distortion from the ideal shape is also evident.

The octagonal geometry was not found for the coordination sphere of a metal atom, but we were able to find two structures that are relatively close (the rightmost points in Figure 3, top), corresponding to the $[MAs_8]^{n-}$ complexes ($M = Nb^V$ or Mo^{VI}),[30] in which the metal atom sits at the center of a nonplanar As_8 ring. Although the shape measures relative to the octagon and to the square antiprism are rather large for these compounds (see Table 3), the path de-

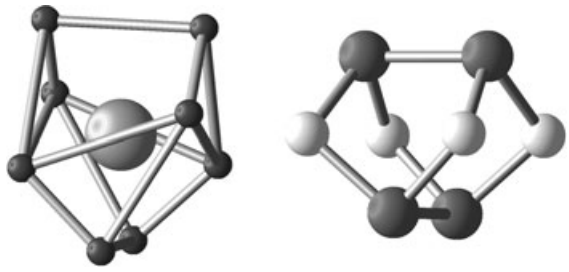

Figure 10. Left: Molecular structure of $[Cd(NO_3)_4]^{2-}$, showing its approximate gyrobifastigium (**GBF**) geometry. Only Cd and O atoms shown for simplicity; the sticks do not correspond to bonds, but are shown to illustrate the edges of the polyhedron. Right: Gyrobifastigium structure of As_4S_4 in realgar, in which the sticks now represent both chemical bonds and polyhedral edges.

Table 3. Shape measures of two As_8^{8-} complexes relative to the octagon (**OP**) and to the square antiprism (**SAPR**), and path deviation functions.

Compound	*S*(OP)	*S*(SAPR)	Δ(OP–SAPR)
$[NbAs_8]^{3-}$	8.13	6.00	0.00
$[MoAs_8]^{2-}$	9.05	5.24	0.00

viation function shows that these structures are right on the path that connects these two polyhedra (deviation functions less than 0.001 in both cases). Note that the two coordination gyrobifastigia and the two compressed square antiprisms occupy the same region in the **SAPR**–**CU** map even though they have two quite different shapes. Thus, the position of a structure in a shape map provides a good hint to the closest polyhedron but not an unequivocal assignment, except for points that are close to the position of either of the two polyhedra used as references in the map.

Edge-bonded polyhedra: In contrast to coordination polyhedra, in which the vertices are held in place through bonds to a central atom, in the edge-bonded polyhedra,[15] the edges correspond to chemical bonds. The most representative case among eight-vertex polyhedra is the long sought for cubane,[31] C_8H_8, as well as its derivatives and Group 14 analogues with Si_8, Ge_8, or Sn_8 skeletons. In this case all the edges are occupied by bonds, but one can conceive polyhedra in which only a fraction of the edges do the job of setting the vertices in place. We call these edge-deficient polyhedra[15] and the prototypical case is the As_4S_4 polyhedron in realgar, in which only ten of the fourteen edges of a gyrobifastigium are occupied by As–S bonds, but which still suffice to organize the eight atoms in the shape of this interesting polyhedron (Figure 10, right). In this section we analyze the shapes of these and related edge-bonded polyhedra.

Cubanes: The cubanes form a wide family of compounds, named after the prototypic alkane C_8H_8, in which the eight vertices of the skeletal polyhedron are connected by 12 direct chemical bonds. In a regular cube the edges meet to form angles of 90°, whereas vertices in cubane are occupied by sp^3 C atoms that prefer bond angles of around 110°. Thus, it is natural to ask how cubic are cubanes? Before answering that question we should distinguish the homocubanes, with all vertices occupied by the same element, and the heterocubanes, M_4X_4, in which alternate vertices are occupied by a metal atom M and a main group element X, such as sulfur or oxygen.

Among the homocubanes with E_8 skeletons, we have retrieved a total of 112 structures with E = C, Al, Si, or Sn. The low values of their shape measures relative to the cube confirm that they are nearly perfect cubes (the CShM values are less than 0.3, and most structures have values below 0.05). Among the transition-metal heterocubanes M_4X_4 we have retrieved 171 oxocubanes (X = O) and 239 thiocubanes (X = S). In this family, significant distortions from the ideal cube are found. The scatterplot of the CShMs relative to **CU** and **TT** reveal a complex stereochemical behavior (Figure 11), with a number of structures close to the perfect

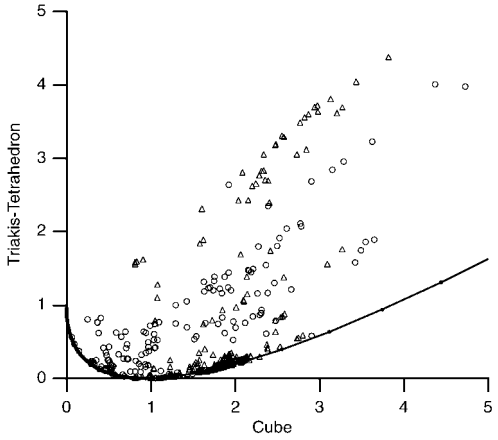

Figure 11. Shape map of heterocubanes relative to the cube and the triakis tetrahedron, showing the M_4O_4 (○) and M_4S_4 (△) transition-metal compounds together with models of compounds of two tetrahedra (● and continuous line), including a cube and a triakis tetrahedron.

cube but also many significantly distorted cubes. Our analysis of such structures in terms of continuous shape measures reveals the presence of two main types of distortions from the ideal cube. In the first type, exhibited by the heterocubanes, the M_4 and X_4 groups retain their tetrahedral shape, but the two tetrahedra differ in size. Let us recall that in the regular cube the two composing tetrahedra are of exactly the same size, whereas the triakis tetrahedron is composed of two tetrahedra whose center-to-vertex distances are in a ratio of 1.218. A representation in the shape map of such a distortion of the cube (Figure 11, continuous line) with retention of the tetrahedral symmetry seems to represent the lower limit for all possible structures, and a large number of experimental structures are found to be practically along that path. The second type of distortion is shown by the large number of structures that significantly deviate from this path. A convenient way to reveal these distortions is to plot the deviation function of the M_4X_4 core from the **CU**–**TT** path as a function of the average of the tetrahedral mea-

sures of its M_4 and X_4 fragments (Figure 12). The deviation from that path correlates well with the deviation of the M_4 and/or X_4 groups from the ideal tetrahedron. In other words, the X atoms asymmetrically bridge three M atoms that form a face of the M_4 tetrahedron.

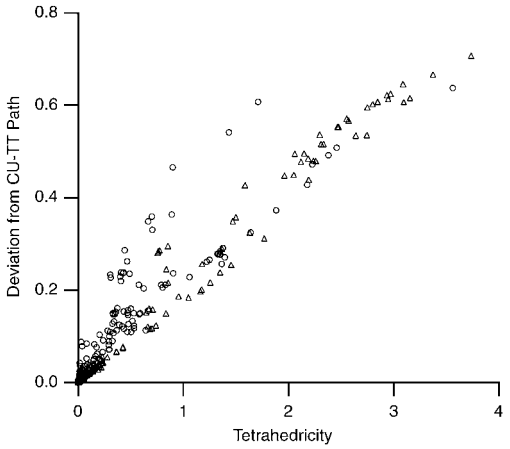

Figure 12. Deviation of M_4O_4 (○) and M_4S_4 (△) heterocubanes from the cube to triakis-tetrahedron interconversion path as a function of the average of the tetrahedral shape measures of the X_4 and M_4 fragments.

Interesting sets of cubes are those that appear in the central Mn_4O_4 core of the single-molecule magnet Mn_{12} compounds, for which 28 structures were found by a CSD search. A CShM analysis of these cores along the same lines applied here for heterocubanes shows unequivocally (Figure 13) that they are significantly distorted from a cube and that such a distortion has to do with local asymmetry rather than with the different sizes of the Mn_4 and O_4 tetrahedra. This type of analysis may be useful for the design of new single-molecule magnets, since the anisotropy of the central core is most likely transmitted toward the exterior of the Mn_{12} molecule, and such anisotropy is of the utmost importance in determining the quantum tunneling properties of these spin systems.

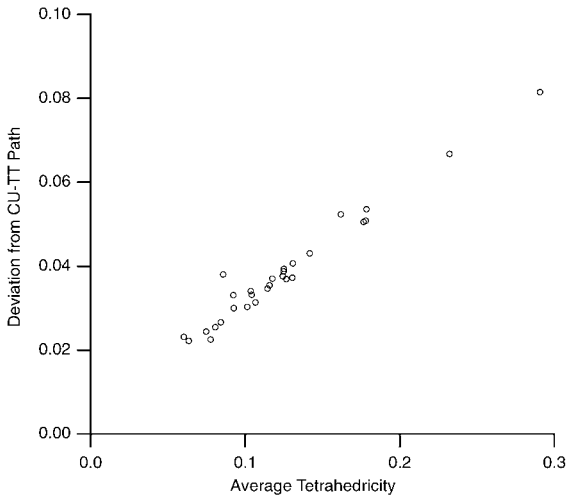

Figure 13. Deviation of the Mn_4O_4 core of the Mn_{12} single-molecule magnet compounds from the cube to triakis-tetrahedron path as a function of the average of the tetrahedral shape measures of the Mn_4 and O_4 fragments.

Gyrobifastigia: The full gyrobifastigium, an eight-vertex polyhedron (**GBF**, Scheme 1), has fourteen edges. We found structural data for only one molecule with fourteen bonds connecting eight atoms that represents a nearly perfect molecular version of this uncommon Johnson polyhedron, namely, $[Cu_8(AsSiMe_3)_4]$,[32] in which the trimethylsilylarsenido ligands cap the square faces of the gyrobifastigium as μ_4 bridges. However, we were able to identify two versions of edge-deficient gyrobifastigia (Table 4), one with ten edge bonds, represented by the As_4S_4 molecules in realgar and by related species such as $P_4(NR)_4$[33] $(Te_4S_4)^{2+}$,[34] $Sb_4(SbR)_4$, and derivatives of tricyclo[3.3.0.$0^{3,7}$]octane (**14**); the 16 such structures found all have CShM values between 8.6 and 9.8, smaller than for other reference polyhedra. The other version has twelve of the fourteen edges formed by chemical bonds, as found in cunneane (pentacyclo[3.3.0.$0^{2,4}$.$0^{3,7}$.$0^{6,8}$]octane, **15**, S(GBF) = 8.8)[35] (Figure 14) In all such molecules, the fact that some edges are chemical bonds (hence short

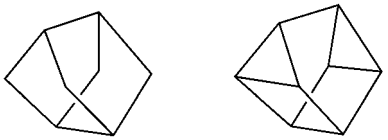

14 **15**

Table 4. Some gyrobifastigia, identified as having S(GBF) smaller than shape measures relative to all other polyhedra considered.

Refcode	Compound	Polyhedron	Edge bonds	S(GBF)
coordination sphere				
BEJFAX	$[Ce(NO_3)_2Cl_4]^{2-}$	$Ce@O_4Cl_4$	0	4.24
IDAWOZ	$[Cd(NO_3)_4]^{2-}$	$Cd@O_8$	0	4.39
edge-bonded polyhedra				
EBUNOE	$[Cu_8(AsSiMe_3)_4]$	Cu_8	14	0.67
	realgar	As_4S_4	10	8.44
	para-realgar	As_4S_4	10	8.36
	P_4S_4	P_4S_4	10	8.72
CEPLOY	$P_4(NtBu)_4$	P_4N_4	10	8.92
GEJMOX	$S_4Te_4^{2+}$	S_4Te_4	10	8.24
NOYWAZ	$C_8H_8O_2$	C_8	10	8.69
RESRUC	cunneane, C_8Me_8	C_8	12	8.78
supramolecular architectures				
YUBLAI	$[Mn_8Sb_4(\mu\text{-}O)_4(\mu\text{-}EtO)_{20}]$	Mn_8	0	0.33

Figure 14. Gyrobifastigium-like carbon skeleton of cunneane, pentacyclo[3.3.0.0^{2,4}.0^{3,7}.0^{6,8}]octane, as found in its octamethyl derivative.[35]

distances) and some others are not bonded (long distances) means that the regularity is perforce lost, and large CShM gyrobifastigium values result. In spite of such large CShM values relative to the gyrobifastigium, they are still significantly smaller than those referred to all other analyzed polyhedra, consistent with their clear gyrobifastigium topology and symmetry.

Square antiprisms: The square antiprism is nicely realized in a Ga_8(fluoren-9-yl)$_8$ cluster[36] in which the 16 edges are formed by Ga–Ga bonds. Its small deviation from the ideal **SAPR** (CShM of 0.22) reflects the differences in distances between the bonds forming the square faces (2.516(5) Å) and those linking these two faces (2.713(5) Å). Although the square antiprism is not a common geometry among transition-metal clusters, the use of the continuous shape measures allowed us to easily identify three examples with nearly perfect square-antiprismatic structure, namely, Ni_8,[37] Ru_8,[38] and Co_8[39] cores that have CShMs relative to the **SAPR** of 0.14, 0.12, and 0.36, respectively.

Octanuclear clusters and supramolecular architectures: In this case, our experimental data come from compounds (in the CSD) with eight transition-metal atoms. A shape map of these structures (Figure 15) reveals more geometric diversity than found among eight-vertex coordination complexes, as seen by comparing the scale of this map with those in Figures 3 and 6. In the present map, one can identify at first sight a structure that is nearly linear, which corresponds to a mixed-valent tetramer of Pt dimers with acetamido bridges,[40] whose CShM value relative to a regularly spaced linear chain of eight atoms is 0.55, which reflects alternating Pt–Pt distances and zig-zag deviation from linearity. In addition, the identification of, for example, the structure of the best molecular gyrobifastigium[41] (Table 4), [Mn_8Sb_4(μ-O)$_4$(μEtO)$_{20}$] (CShM = 0.33), as well as a variety of octagonal M_8 groups, such as Cr_8 in [Cr_8F_8(pivalato)$_{16}$][42] (Figure 16), are good examples of the stereochemical diversity. A variety of square antiprismatic and dodecahedral structures are found in our reference structural set, with varying degrees of distortion from the ideal polyhedra. Another interesting case of octanuclear architecture is that of the FeMo cofactor in nitrogenase, which forms a Fe_7Mo cluster[43] with nearly perfect **J-ETBP** geometry (CShM = 0.02).

Inorganic solids: In this section we present an analysis of the atomic coordination geometry in several representative

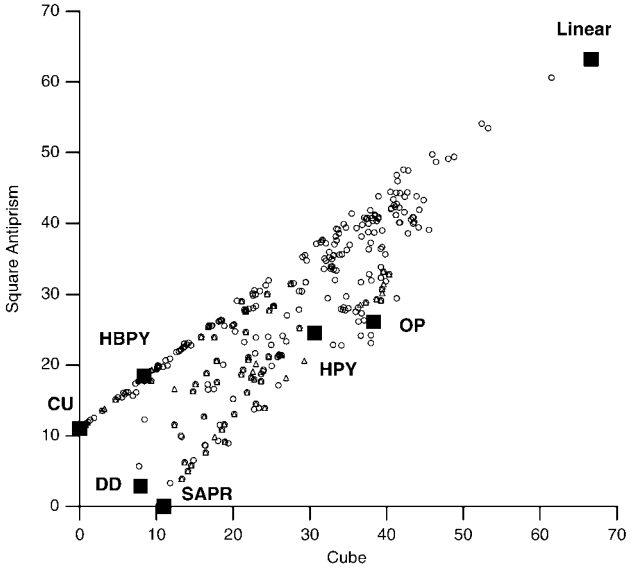

Figure 15. Shape map relative to the cubic and square antiprismatic shape measures of octanuclear transition-metal compounds, differentiating those that are connected in a cyclic way (△) from those that are not (○). Some reference polyhedra are indicated by solid squares (see Scheme 1 for abbreviations).

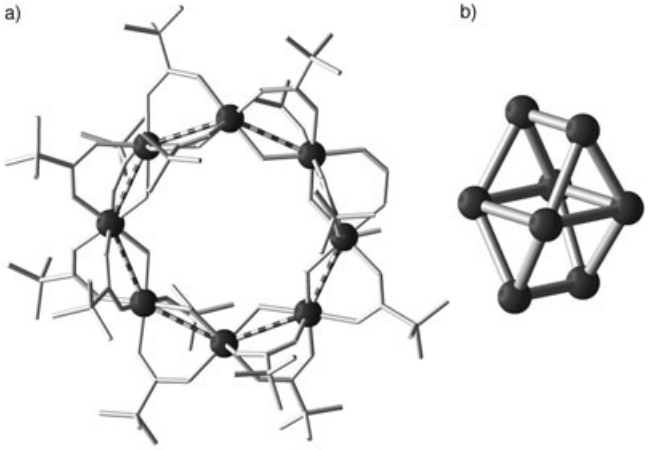

Figure 16. Supramolecular octogonal architecture of the Cr_8 group in a) [Cr_8F_8(pivalato)$_{16}$] and b) gyrobifastigium of the Mn_8 skeleton in [Mn_8Sb_4(μ-O)$_4$(μ-Et)$_{20}$].[41,42]

structures of extended solids. As expected, for structures in which the cations occupy a crystallographic site with strictly cubic symmetry, such as the rock salt and fluorite structures, the cubic shape measures are zero within numerical accuracy, as seen in Table 5 for such compounds as CsCl, NaTl, CaF_2, ScH_2, UO_2, and ThO_2.

Although in most cases the polyhedral classifications reflected in the classical review of Lippard[11] are confirmed and put on a quantitative scale by our shape measures, the earlier description of some of those structures is clearly changed when a proper continuous shape measure analysis is carried out. This is the case for ZrF_4 and $ZrOCl_2{\cdot}8H_2O$, for which a square antiprismatic structure was proposed, yet

Table 5. Shape measure of the closest polyhedron for a sample of octacoordinate atoms in extended solid state structures.

Atom	Compound	CShM	Atom	Compound	CShM
	cube: **CU**			bicapped trigonal prism: **J-BTP** (**s-BTP**)	
Cs	CsCl	0.00	C	Fe_3C	0.26 (0.83)
Na	NaTl	0.00	Ta	$TaAs_2$	2.53, 2.68 (1.69)
Ca	CaF_2	0.00	Mo	$MoAs_2$	2.63 (1.83)
Sc	ScH_2	0.00	Os	$OsGe_2$	2.64 (1.87)
U	UO_2	0.00	Cr	$CrAs_2$	2.71 (1.78)
Th	ThO_2	0.00	V	VP_2	2.78 (1.95)
			Cr	CrP_2	2.93 (2.07)
			W	WP_2	3.09 (2.16)
	elongated trigonal pyramid: **s-ETBP**				
Re	ReB_2	0.03			
	dodecahedron: **DD**			square antiprism: **SAPR**	
Zr	ZrF_4	0.60	Zr	$Zr(IO_3)_4$	0.08
Zr	$ZrOCl_2(H_2O)_8$	0.63	Ta	Na_3TaF_8	0.14
Zr	$Li_6BeF_4ZrF_8$	0.89	Hf	HfF_4	0.22
Zr	$Zr(SO_4)_2{\cdot}5H_2O$	0.91	Re	K_2ReF_8	0.27
Os	Os_4Sn_{17}	1.35	Cu	$CuAl_2$	0.34
Zr	$ZrSiO_4$	1.67	Nb	$NbSn_2$	0.42
Ti	$Ti(NO_3)_4$	2.00	Rh	$RhSn_3$	0.45
	snub disphenoid: **SD**		Co	$CoIn_2$	0.76
C	ScC_3	0.51	Zr	K_2ZrF_6	0.83
			Hf	$HfF_4{\cdot}3H_2O$	1.03
			Hf	$HfGe_2$	2.89

we find their dodecahedral shape measures (0.60 and 0.63, respectively) to be much smaller than the corresponding antiprism measures (2.49 and 2.23, respectively). Another interesting case is that of $HfF_4{\cdot}3H_2O$, which was classified as a square antiprism, whereas our shape measures of S(SAPR) = 1.03 and S(DD) = 1.85 point to significant distortion from the antiprism. The deviation function from the **DD–SAPR** interconversion path for this compound gives a practically negligible value (0.005) and clearly classifies such a coordination polyhedron as intermediate between the dodecahedron and the square antiprism, albeit slightly closer to the antiprism. It is easy to find the bicapped trigonal prism as a coordination polyhedron among solid-state compounds (see Table 5), but these deviate significantly from the ideal polyhedron because of the existence of element–element bonds between some of the vertices. For example, in $CrAs_2$ the As atoms form $(As^0)_8$ layers of fused hexagons and $(As^-)_8$ chains. Thus, there are three quite different edges of the **BTP** coordination polyhedron (Figure 17):

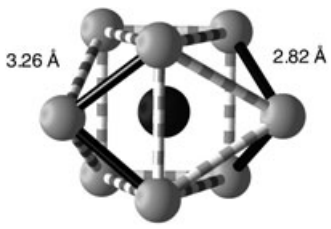

Figure 17. **BTP** coordination sphere of the Cr atom in $CrAs_2$. The black cylinders correspond to chemical bonds, whereas the striped ones are only shown to highlight the coordination polyhedron.

those of the capping triangular faces that correspond to As–As bonds (ca. 2.7 Å), the edges of the tetragonal faces bridged by As_3 moieties (ca. 3.3 Å), and the edges corresponding to the bases of the trigonal prism, which are nonbonded As···As distances (ca. 3.7 Å), and the resulting significant distortion from the ideal Johnson polyhedron is reflected in an S(J-BTP) value of 2.71.

An apparently uncommon shape that we can find among the solids is the **ETBP**, as in ReB_2, which is also uncommon among the octacoordinate structures in molecular complexes discussed above. The large CShM value found for the coordination sphere of Re in this compound relative to the Johnson polyhedron, S(J-ETBP) = 6.86, results because it is much closer to the spherical version of the elongated trigonal bipyramid with all Re–B distances the same (see Table 5). However, even if we use only the Johnson reference polyhedron, the comparison of this CShM value with the shape measures relative to all other reference polyhedra, all of which exceed 20 units, clearly shows that the geometry of the ReB_8 core is **ETBP**.

An illustrative example of how a combination of continuous shape measures and path deviation functions can provide an excellent stereochemical description of the coordination sphere of a given atom in an extended solid can be found in $Y_2Ti_2O_7$. In this compound, the Y atom is coordinated by eight oxygen atoms. Its smallest shape measures relative to eight-vertex polyhedra are those for the cube (2.10) and the hexagonal bipyramid (2.93). Since these values are still large enough to indicate significant distortion from either ideal shape, we look at its deviation from the corresponding interconversion path, whose small value (0.08) allows us to describe its geometry as intermediate between the cube and the hexagonal bipyramid.

Another example is provided by the garnet structure, as pointed out by O'Keeffe and Hyde.[1] Garnets have the general formula $A^{II}_3M^{III}_2(SiO_4)_3$, where A^{II} can be Ca, Sc, Mg, Fe, or Mn, and M^{III} can be Al, Cr, or Fe. These authors stressed that the coordination geometry of the A^{II} ions in the garnet structure is described by different authors as a "skew cube", a "distorted square antiprism", or a "distorted dodecahedron". Let us see how the continuous shape measures can handle such a situation. To that end, we analyzed the alkaline earth coordination sphere in a sample of garnet structures (Table 6). In none of these cases do the shape measures allow one to unequivocally assign an ideal poly-

Table 6. Shape measures and path deviation functions for the coordination sphere of the divalent cation in some garnets.

Garnet	CU	SAP	DD	Δ(CU–SAP)	Δ(CU–DD)
almandine	2.59	3.44	3.04	0.04	0.18
andradite	2.73	3.28	3.05	0.03	0.20
blythite	2.58	3.35	3.01	0.02	0.17
calderite	2.60	3.33	3.02	0.02	0.18
grossular	2.87	3.36	3.12	0.05	0.22
kaotite	2.56	4.72	3.82	0.12	0.25
knorringite	2.48	3.43	3.01	0.02	0.16
majorite	2.45	3.44	3.03	0.02	0.16
pyrope	2.64	3.41	3.04	0.03	0.18
skiagite	2.53	3.39	3.02	0.02	0.17
uvarovite	2.84	3.27	3.08	0.04	0.21

hedral shape to the AO_8 core, as seen by CShM values relative to the cube, the square antiprism, and the dodecahedron between 2.4 and 4.7 (Table 6). However, in all cases the deviation functions from the **CU**–**SAPR** path have small enough values (the largest deviation from that path is 0.12) to indicate that the coordination polyhedra are well described as intermediate between the cube and the square antiprism, also called square metaprisms. Interestingly, in the analyzed garnets there is little variation in the degree of distortion from the cube. Another interesting observation for the cases of andradite and grossular, for which X-ray diffraction structures have been reported at different temperatures,[44] is that the AO_8 metaprisms rotate toward the cube as the temperature is lowered (Figure 18).

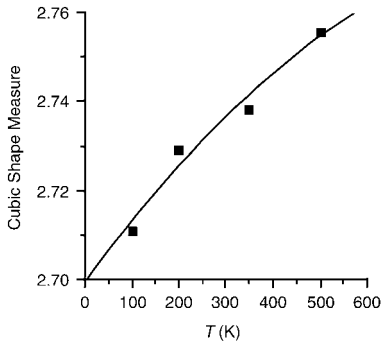

Figure 18. Changes in the cubic shape measure of the Ca^{II} environment in andradite as a function of temperature.

Conclusion

We have adopted eleven eight-vertex polyhedra as reference shapes to gauge the stereochemisry of a variety of molecular structures and substructures by using continuous shape measures. In the shape space, there is a region in which several such polyhedra are grouped: the triangular dodecahedron, the snub disphenoid, the square antiprism, and the bicapped trigonal prism, coincident with the polyhedra that were classified by Muetterties as low-energy geometries for coordination compounds. In another region we find the cube and the triakis-tetrahedron, and all the remaining ideal polyhedra are scattered at large distances from these two regions and from each other: the hexagonal bipyramid, the gyrobifastigium, the elongated trigonal bipyramid, the heptagonal pyramid, and the octagon.

For some polyhedra there is no unique definition of ideality. In these cases we chose two alternative reference shapes: the Johnson polyhedra, wherein all edges have the same length but different distances from vertex to center, and the spherical polyhedra, in which all such distances are identical but not all the edges are equal. According to our analysis of several families of compounds, we conclude that the Johnson polyhedra seem best suited to define the geometries of clusters and supramolecular architectures, whereas their spherical counterparts are more adequate to describe atom coordination spheres.

The analysis of the experimental structures of transition-metal coordination compounds indicates that octacoordination is most common among the early second- and third-row transition metals and for Zn and Cd. Their stereochemical distribution is dominated by the low-energy polyhedra (**DD**, **BTP**, and **SAPR**), intermediate geometries, and geometries along the path from those polyhedra toward the **HBPY**. Small but significant numbers of structures correspond to cubes (3.8%) and hexagonal bipyramids (4.1%). The stereochemical preferences show some differences for the metal ions with d^0 to d^2 electron configurations and those with the d^{10} configuration. While the former are scattered around the low-energy polyhedra, with some clearly tracing the **SAPR**–**DD** interconversion path, the latter are not found in dodecahedral geometry. Some structures of coordination complexes were also classified according to their ligands, and the stereochemical preferences that emerge are schematically summarized in Figure 9.

The homocubanes of C, Al, Si, or Sn are nearly perfectly cubic. In contrast, significant distortions from the cube can be found among the M_4X_4 heterocubanes, which can be attributed either to the combination of M_4 and X_4 nearly-perfect tetrahedra of different sizes or to the deviation of one or both of these components from tetrahedricity.

Studying the shape measures of the coordination spheres of metal atoms in ionic solids allowed us to detect in some cases imprecise assignments of coordination polyhedra. For example, application of the path deviation functions showed that the Y atom in $Y_2Ti_2O_7$ lies precisely along the path from the cube to the hexagonal bipyramid, at similar distances from these two ideal polyhedra. Similarly, the coordination environment of the divalent ions in the garnet structures can be precisely described as square metaprisms, intermediate between the cube and the square antiprism.

In summary, we have shown that we can describe within the same framework of continuous shape measures and path deviation functions the structures of a wide variety of eight-vertex chemical systems in an accurate way. We have also shown how easily one can detect unusual structures at a glance in a shape map. Thus, we have identified several structures that are nicely described by the thus far neglected

gyrobifastigium, as in two coordination compounds, $[Ce(NO_3)_2Cl_4]^{2-}$ and $[Cd(NO_3)_4]^{2-}$, in the As_4S_4 realgar structure, in some inorganic and organic analogues such as cunneane, in a Mn_8 supramolecular compound, and in a Cu_8 cluster. Similarly we identified a Cr_8 octagon and the geometries of two $[MAs_8]^{n-}$ compounds, intermediate between the octagon and the square antiprism, square antiprismatic structures of Ga_8, Ni_8, Ru_8 or Co_8 clusters, and a nearly perfect elongated trigonal bipyramid in the Fe_7Mo cluster of nitrogenase.

Acknowledgements

This work has been supported by the Ministerio de Ciencia y Tecnología, projects BQU2002-04033-C02-01 and BQU2002-04033-C02-02, and by Comissió Interdepartamental de Ciència i Tecnologia (CIRIT), grant 2001SGR-0044.

[1] M. O'Keeffe, B. G. Hyde, *Crystal Structures. I. Patterns and Symmetry*, Mineralogical Society of America, Washington, D.C., **1996**.
[2] H. Zabrodsky, S. Peleg, D. Avnir, *J. Am. Chem. Soc.* **1992**, *114*, 7843.
[3] M. Pinsky, D. Avnir, *Inorg. Chem.* **1998**, *37*, 5575.
[4] J. Cirera, P. Alemany, S. Alvarez, *Chem. Eur. J.* **2004**, *10*, 190.
[5] S. Alvarez, D. Avnir, M. Llunell, M. Pinsky, *New J. Chem.* **2002**, *26*, 996.
[6] D. Casanova, J. M. Bofill, P. Alemany, S. Alvarez, *Chem. Eur. J.* **2003**, *9*, 1281.
[7] D. Casanova, J. Cirera, M. Llunell, P. Alemany, D. Avnir, S. Alvarez, *J. Am. Chem. Soc.* **2004**, *126*, 1755.
[8] E. L. Muetterties, C. M. Wright, *Q. Rev. Chem. Soc.* **1967**, *21*, 109.
[9] J. K. Burdett, R. Hoffmann, R. C. Fay, *Inorg. Chem.* **1978**, *17*, 2553; D. L. Kepert, *Inorganic Stereochemistry*, Springer, New York, **1982**.
[10] D. L. Kepert, *Adv. Inorg. Chem.* **1978**, *24*, 179.
[11] S. J. Lippard, *Prog. Inorg. Chem.* **1967**, *8*, 109.
[12] D. L. Kepert in *Comprehensive Coordination Chemistry*, *Vol. 1* (Eds.: G. Wilkinson, R. D. Gillard, J. A. McCleverty), Pergamon, Oxford, **1987**, p. 31; B. W. Clare, D. L. Kepert in *Encyclopedia of Inorganic Chemistry*, *Vol. 2* (Ed.: R. B. King), Wiley, Chichester, **1994**, p. 795.
[13] J. G. Leipoldt, J. S. Basson, A. Roodt, *Adv. Inorg. Chem.* **1993**, *40*, 241.
[14] H. Zabrodsky, S. Peleg, D. Avnir, *J. Am. Chem. Soc.* **1993**, *115*, 7843 (Erratum: **1994**, 116, 656).
[15] S. Alvarez, *An. Real Soc. Esp. Quím.* **2003**, *99*, 29.
[16] P. R. Cromwell, *Polyhedra*, Cambridge University Press, Cambridge, **1997**.
[17] More information and interactive views of these polyhedra can be found on the internet at http://mathworld.wolfram.com/topics/Polyhedra.html.
[18] V. Pfennig, N. Robertson, K. Seppelt, *Angew. Chem.* **1997**, *109*, 1410; *Angew. Chem. Int. Ed. Engl.* **1997**, *36*, 1350.
[19] M. J. Bennett, F. A. Cotton, P. Legzdins, S. J. Lippard, *Inorg. Chem.* **1968**, *7*, 1770.
[20] J. Szkalrzewicz, A. Samotus, B. Nowicka, J. Burgess, J. Fawcett, D. R. Russell, *Transition Metal Chem.* **1999**, *24*, 177.
[21] F. H. Allen, O. Kennard, *Chem. Des. Autom. News* **1993**, *8*, 31.
[22] E. M. Larsen, G. N. LaMar, *J. Chem. Educ.* **1974**, *51*, 633; J. K. Burdett, *Molecular Shapes*, Wiley, New York, **1980**.
[23] J. Liu, Z. Song, L. Wang, J. Zhuang, X. Huang, *Acta Chem. Scand.* **1999**, *53*, 90; A. A. Naiini, V. Young, J. G. Verkade, *Polyhedron* **1995**, *14*, 393; R. Wietzke, M. Mazzanti, J.-M. Latour, J. Pecaut, *Chem. Commun.* **1999**, 209.
[24] Z. Wang, K. Sakata, M. Hashimoto, *Polyhedron* **1998**, *17*, 4451.
[25] G. S. Papaefstathiou, S. P. Perlepes, A. Escuer, R. Vicente, M. Font-Bardía, X. Solans, *Angew. Chem.* **2001**, *113*, 908; *Angew. Chem. Int. Ed.* **2001**, *40*, 884; A. Tsohos, S. Dionyssopoulou, C. P. Raptopoulou, A. Terzis, E. G. Bakalbassis, S. P. Perlepes, *Angew. Chem.* **1999**, *111*, 1036; *Angew. Chem. Int. Ed.* **1999**, *38*, 983.
[26] J. Pickardt, G.-T. Gong, I. Hoffmeister, *Z. Naturforsch. B: Chem. Sci.* **1995**, *50*, 993.
[27] J. Pickardt, B. Kuhn, *Z. Naturforsch. B: Chem. Sci.* **1994**, *49*, 1031.
[28] K. S. Hagen, *Angew. Chem.* **1992**, *104*, 804; *Angew. Chem. Int. Ed. Engl.* **1992**, *31*, 764.
[29] A. Brandt, Y. M. Kiselev, L. I. Martynenko, *Zh. Neorg. Khim.* **1981**, *26*, 2950; U. Rajalingam, P. A. W. Dean, H. A. Jenkins, M. Jennings, J. M. Hook, *Can. J. Chem.* **2001**, *79*, 1330.
[30] H. G. von Schnering, J. Wolf, D. Weber, R. Ramirez, T. Meyer, *Angew. Chem.* **1986**, *98*, 372; *Angew. Chem. Int. Ed. Engl.* **1986**, *25*, 353; B. W. Eichhorn, S. P. Mattamana, D. R. Gardner, J. C. Fettinger, *J. Am. Chem. Soc.* **1998**, *120*, 9708.
[31] A. Nickon, E. F. Silversmith, *Organic Chemistry, the Name Game*, Pergamon Press, New York, **1987**.
[32] J. Besinger, D. Fenske, *Z. Anorg. Allg. Chem.* **2001**, *627*, 1487.
[33] D. DuBois, E. N. Duesler, R. T. Paine, *J. Chem. Soc. Chem. Commun.* **1984**, 488.
[34] R. Faggiani, R. J. Gillespie, J. E. Verkris, *J. Chem. Soc. Chem. Commun.* **1988**, 902.
[35] H. Irngantinger, S. Strack, R. Gleiter, S. Brand, *Acta Crystallogr. Sect. C* **1997**, *53*, 1145.
[36] A. Schnepf, G. Stosser, H. Schnockel, *Z. Anorg. Allg. Chem.* **2000**, *626*, 1676.
[37] A. Ceriotti, G. Longoni, M. Manassero, M. Perego, M. Sansoni, *Inorg. Chem.* **1985**, *24*, 117.
[38] L. M. Bullock, J. S. Field, R. J. Haines, E. Minshall, M. H. Moore, F. Mulla, D. N. Smit, L. M. Steer, *J. Organomet. Chem.* **1990**, *381*, 429.
[39] V. G. Albano, P. Chini, G. Ciani, S. Martinengo, M. Sansoni, *J. Chem. Soc. Dalton Trans.* **1978**, 463.
[40] K. Sakai, K. Matsumoto, *J. Am. Chem. Soc.* **1989**, *111*, 3074.
[41] U. Bemm, R. Norrestam, M. Nygren, G. Westin, *Inorg. Chem.* **1995**, *34*, 2367.
[42] N. V. Gerbeleu, Y. T. Struchkov, G. A. Timko, A. S. Batsanov, K. M. Indrichan, G. A. Popovich, *Dokl. Akad. Nauk SSSR* **1990**, *313*, 1459.
[43] O. Einsle, F. A. Tezcan, S. L. A. Andrade, B. Schmid, M. Yoshida, J. B. Howard, D. C. Rees, *Science* **2002**, 297, 1696.
[44] T. Armbruster, C. A. Geiger, *Eur. J. Miner.* **1993**, *5*, 59; C. A. Geiger, T. Armbruster, *Am. Miner.* **1997**, *82*, 740; U. Rodehorst, C. A. Geiger, T. Armbruster, *Am. Miner.* **2002**, *87*, 542.

Received: August 4, 2004
Published online: January 18, 2005